Motional Heterogeneity in Poly(ether-*block*-amide) Copolymers As Revealed by Solid-State NMR

Catherine Hucher,[†] René-Paul Eustache,[†] François Beaume,[†] and Piotr Tekely*[,‡]

ARKEMA, Centre d'Etude de Recherche et Développement, 27470 Serquigny, France, and Methodologie RMN UMR CNRS 7565, Université H. Poincaré, 54506 Vandoeuvre-lès-Nancy, France

Received July 25, 2005; Revised Manuscript Received September 8, 2005

ABSTRACT: An insight into the motional heterogeneity of a series of poly(ether-*block*-amide) copolymers is presented and discussed in terms of its NMR fingerprints dependent on a content and length of hard and soft segments and a microphase-separated morphology. Local-field dipolar spectra carry a straightforward signature of microphase-separated morphology endowed with a strong mobility gradient. The dipolar features of the poly(tetramethylene glycol) (PTMG) and polyamide-12 (PA) components, besides visualizing the presence of separated PTMG and PA phases, also give evidence for the presence of the dynamic heterogeneity of each component. ^{1}H MAS spectra provide an another fingerprint of phase-separated systems. Although such spectra roughly show increasing line broadening at higher PA/PTMG ratio, they are mainly sensitive to the presence of the most mobile fragments and may give a distorted vision of intrinsic mobility of the soft component in the presence of its dynamic heterogeneity. ^{13}C spectra bearing proton−carbon *J*-coupling features appear to be more sensitive to the length of the soft blocks and seem to bring a proper visualization of their overall mobility. Special attention has been paid to characterize motional heterogeneity of the soft component by exploiting cross-polarization transfer efficiency combined with indirect $T_2(^1\mathrm{H})$ relaxation measurements. The cross-polarization inversion experiments provide, from heteronuclear dipolar interaction perspective, a corroborating visualization of the extent of motional distribution of the PTMG component. The revealed fingerprints of the motional heterogeneity of the soft component and the ways exploited in this work for their retrieval might be helpful for a better assessment of its role in the mechanical properties of thermoplastic elastomers.

Introduction

There is still a great deal of interest in the study of block copolymers known for a wide range of industrial applications. Block copolymers with immiscible soft and rigid blocks can form various microphase-separated, mostly complicated nanostructures, providing materials with a useful combination of elasticity and mechanical strength.

Poly(ether-*block*-amide) (PEBA) thermoplastic elastomers are block copolymers having alternating sequences of hard polyamide (PA) and soft polyether (PE) segments and a microphase-separated morphology.[1] At the normal service temperatures the rigid part acts as a physical cross-link site for the rubbery phase of the soft blocks. By changing the polyamide (PA6, PA6.6, PA11, PA12, etc.) and the polyether segment (PTMG, PEG, PPG, etc.), the mechanical, chemical, and physical properties can be conveniently modeled.[1] Some aspects of the phase structure, morphology, and the basic physicochemical properties of poly(ether-*block*-amides) have been studed by transmission electron[2] and atomic force microscopies,[3,4] small-[3b,4] and wide-angle X-ray scattering,[4,5] small-angle light scattering,[4] and differential scanning calorimetry[2,4−6] as well as by dynamic mechanical analysis[1b,4,5,7] and thermally stimulated current methods.[8]

Solid-state NMR spectroscopy is now recognized as one of the most powerful tools for structural and dynamic studies of polymeric materials. Several research groups used indeed solid-state NMR methods, based on proton spin-diffusion phenomena, to investigate the phase structure and to determine the rigid and mobile domain sizes on the nanometer length scale (typically between 2 and 30 nm) as well as the sizes of interphases (0.5−2.5 nm) in a number of block copolymers.[9−21] Some attention has been also paid to the investigation of molecular mobility of block copolymers by proton,[10] deuterium,[22−25] and carbon-13 [17,26−29] solid-state NMR techniques.

Somewhat surprisingly, no any systematic solid-state NMR study of the poly(ether-*block*-amide) copolymers has been published yet. As far as we know, only standard ^{13}C and ^{15}N CP/MAS spectra of a few poly(ether-*block*-amide) copolymers have been presented and discussed in terms of their chemical structure and polymorphic features of the crystalline polyamide phase.[30,31] The principal aim of our work is to probe the motional heterogeneity in poly(ether-*block*-amide) copolymers which is supposed to play an important, albeit still not well recognized, role in the mechanical properties of block copolymers.[1] We give first an insight into the overall molecular mobility of a series of structurally different samples against the content and length of hard and soft segments. To gain a deeper insight into the motional heterogeneity of the soft component, we exploit an approach based on the cross-polarization transfer efficiency combined with different well-established methods of high-resolution solid-state ^{13}C NMR spectroscopy.

Experimental Part

Polymers. Poly(ether-*block*-amide) copolymers, commercialized by Arkema under the trademark Pebax, and available in granular form, were cryomilled at liquid nitrogen temperature. To avoid the influence of thermal and process history on the morphology, each sample has been subsequently dried

[†] ARKEMA.
[‡] Université H. Poincaré.
* Corresponding author: e-mail Piotr.Tekely@rmn.uhp-nancy.fr; Fax (33) 383684347; Tel (33) 383684352.

10.1021/ma051625q CCC: $30.25
Published on Web 10/07/2005

Table 1. Molecular Characteristics of Block Polyamide (PA) and Poly(tetramethylene glycol) (PTMG) Copolymers Studied

sample no.	av block length PA/PTMG, g mol^{-1}	av block length ratio
1	600/2000	0.3
2	850/2000	0.425
3	2000/2000	1.0
4	1000/1000	1.0
5	2000/1000	2.0
6	4000/1000	4.0
7	5000/650	7.69

overnight under vacuum at 80 °C. Seven copolymers with varying composition and block length were investigated by NMR (Table 1).

Solid-State NMR Experiments. All NMR experiments were carried out on a Bruker DSX 300 spectrometer. The operating frequencies were 300.13 MHz for ^{1}H and 75.47 MHz for ^{13}C. Cross-polarization magic-angle spinning (CP/MAS) spectra have been recorded at a spinning frequency of 4 kHz with carrefully adjusted and supervised $n = -1$ Hartmann−Hahn cross-polarization conditions, i.e., $\nu_{1H} = \nu_{1C} - \nu_r$. ^{1}H MAS spectra were acquired at a spinning frequency of 4 kHz. Several relaxation measurements probing a large frequency scale of molecular motions have been performed. Indirect measurements of proton $T_{1\rho}$ relaxation times have been conducted with standard variable spin-lock period ($\nu_{1H} = 62.5$ kHz) preceding the cross-polarization contact time. The ^{13}C spin−lattice relaxation times in the laboratory frame were measured by the method of Torchia.[32]

Results and Discussion

Among the main parameters defining the physicochemical properties of poly(ether-*block*-amide) copolymers, three of the most important are the chemical nature of each block, the weight ratio PA/PTMG, and the length of each block. These parameters determine the glass and melting temperature, the chemical resistance, the mechanical properties like stiffness and elasticity, and the degree of segregation of the two chemical components. In polymers well above T_g, molecular motions reduce considerably the broadening effect arising from the anisotropic interactions undergone by nuclear spins. In the case of poly(ether-*block*-amide) copolymers, this is the case of the soft component for which the observed residual line widths are due to rapid anisotropic segmental motion hampered by chain constrains such as covalent linking to PA block, the presence of PA crystalline domains behaving as virtual cross-links, and the possible partial miscibility of both components, all three acting as anchors for the rapid segmental reorientations.

In this work we wish to get an insight into the degree of molecular mobility and its changes in a series of poly(ether-*block*-amide) copolymers probing different types of spectral broadening arising from dipolar or scalar interactions as well as different types of relaxation measurements. To provide a dynamic framework for these studies in relation to the chemical structure composition, we will start with a short resume of some salient motional characteristics from the dynamic mechanical analysis.

1. Overview of Molecular Mobility and Microphase Separation by Dynamic Mechanical Analysis. The position and origin of dynamic mechanical analysis (DMA) relaxation regions observed in poly(ether-*block*-amide) copolymers have been already discussed in the literature.[1b,4,5,7] Figure 1 shows the evolution of tan δ as a function of temperature for various PA/PTMG mole ratios. Each relaxation is accompanied by a peak in the tan δ curve, the multiple relaxations being labeled α, β, and γ, when going from higher to lower temperatures. The γ peak present below −100 °C is attributed to local motions of the CH_2 groups inside the polyamide and polyether phases and remains very similar for all compositions. The β region placed between −80 and −50 °C is supposed to be the sum of two relaxation processes: the first relaxation is the glass transition of the PTMG-rich phase (about −80 °C) and is clearly predominant for soft and medium grades (samples **1**, **2**, **3**, and **5**). This relaxation, having essentially the same position for this range of PA/PTMG ratios, can overlap with a secondary relaxation from local motions of free and water bound amide groups, very well known in the polyamides and easily observed in the rigid grades **7** and **8** (PA/PTMG = 20). The α region between −20 and +40 °C is attibuted to the glass transition of the polyamide phase (+50 °C for the pure PA). This relaxation can overlap with another relaxation due to the melting of the PTMG; however, the samples investigated by NMR in this work did not contain any crystalline phase of the PTMG component. One can note that, except for samples **7** and **8**, the maximum position of the glass transition relaxation of the PA is placed well below the room temperature and decreases for a lower PA/PTMG ratio. The existence of two, well-separated, glass transitions from the amorphous polyamide and polyether corroborates a well-defined microphase separation within the amorphous part of poly(ether-*block*-amide) copolymers. The observed lowering of the glass temperature of the PA component at lower PA/PTMG ratios has most probably for origin a combined effect from different scenarios like increasing role of internal plasticization due to the presence of oligoamide components inside the polyamide regions for samples with shorter PA blocks, the related progressive disruption of the hydrogen-bond contacts, and possible external plastization due to increasing effect of growing soft polyether matrix covalently bonded to the polyamide segments.[1,6] The presence of mixed PA/PTMG phase has also been suggested in the literature.[2,4]

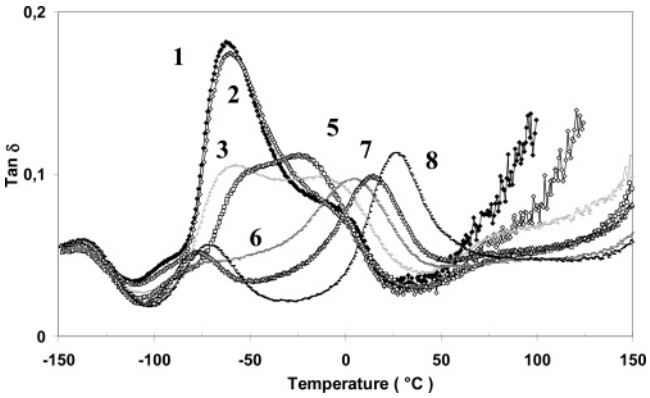

Figure 1. Evolution of tan δ as a function of temperature for various PA/PTMG mole ratios (sample **8** has a PA/PTMG mole ratio 5000/250).

2. Overview of Molecular Mobility and Phase Structure by Solid-State NMR. *Local Field Features of Soft and Rigid Components.* It has been shown previously that the popular WISE experiment[33] used commonly to investigate site-resolved molecular mobilities in heterogeneous polymeric materials may be further exploited to obtain dipolar local field spectra providing local structural and dynamic information.[34]

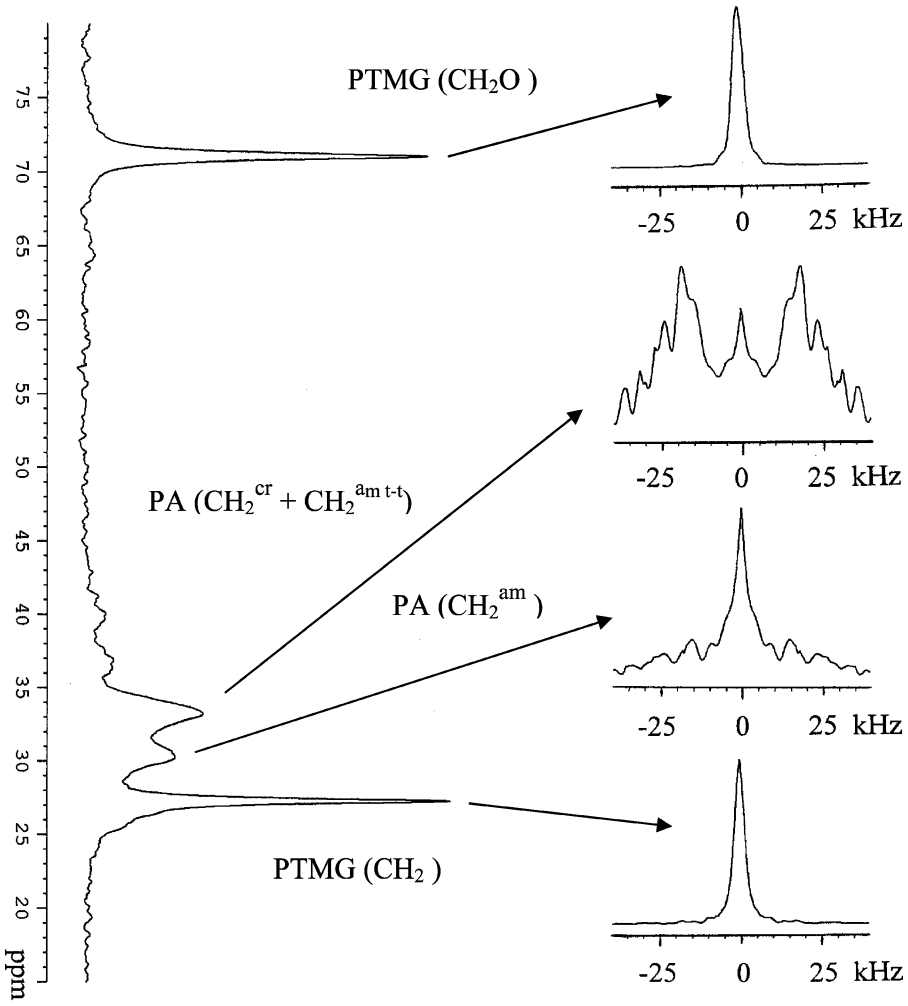

Figure 2. Dipolar slices of methylene groups separated according to the ^{13}C chemical shift from different positions in the chain of sample **2** and recorded using contact time of 30 μs and ν_r = 4 kHz. 32 increments of 2 μs were used in t_1, and the imaginary part of the transposed FID was set to zero in order to symmetrize the dipolar spectra.

The success of this local-field experiment relies on the effective isolation of the protons directly bonded to the carbon-13 nucleus. In fact, the resonance frequency for a proton spin $^1H^*$ coupled to a ^{13}C atom is different from those for ^1H spins coupled to ^{12}C, and this leads to a slower flip-flop exchange between the $^1H^*$ and other ^1H spins.[35] Moreover, for elastomers well above T_g, high molecular mobility reduces dipolar interactions dramatically, and spin diffusion is much less effective than in the glassy or crystalline state.[36] Both factors lead to a greatly diminished role for proton−proton flip-flops. Consequently, using a very short period of polarization transfer, the effective number of spins can be restricted to the nearest neighbors that govern the dipolar local field interactions which are subsequently unravelled in the ν_1 cross sections. In the absence of molecular motions these dipolar slices provide structural information on internuclear distances while their collapse may be used to detect the presence of large-amplitude molecular motions with frequencies comparable to or greater than the dipolar line width.[34,36]

As an example, Figure 2 shows dipolar slices of methylene groups separated according to the ^{13}C chemical shift from different positions in the chain of sample **2**. Further dipolar cross sections are given in Figure 3 for the PTMG $-OCH_2-$ and amorphous PA $-CH_2-$ resonances from four other samples representive of a whole range of chemical structures investigated in this work. A dramatic difference in the shape and line width of methylene groups belonging to PTMG and PA blocks is immediately observed in these two figures. This is a clear fingerprint of phase-separated systems endowed with a strong mobility gradient. Dipolar cross sections from the crystalline and amorphous PA also show a huge difference with a characteristic ~32 kHz splitting from the rigid $-CH_2-$ group and a much narrower dipolar line width, respectively. This permits a favorable observation of the line shape from the amorphous PA, which visualizes in all but one case a complex character indicative of its dynamic heterogeneous nature. Equally interesting for this work, the apparent two-component character of dipolar slices in Figure 3 gives also first indication for the inhomogeneous dynamic character of the PTMG blocks.

We wish to point out that despite common belief that only proton−proton dipolar couplings manifest themselves in the first dimension of the WISE experiment, both homonuclear and heteronuclear dipolar effects determine the dipolar cross sections, especially when recorded with short contact time.[34,36] The heteronuclear dipolar effects may be suppressed by decoupling irradiation applied to the carbon channel during the t_1 period.[37] Finally, it is worth taking note that in order to access the local field features of the soft and rigid components, a very short contact time of 30 μs has been used in these experiments. Consequently, the observed dipolar line

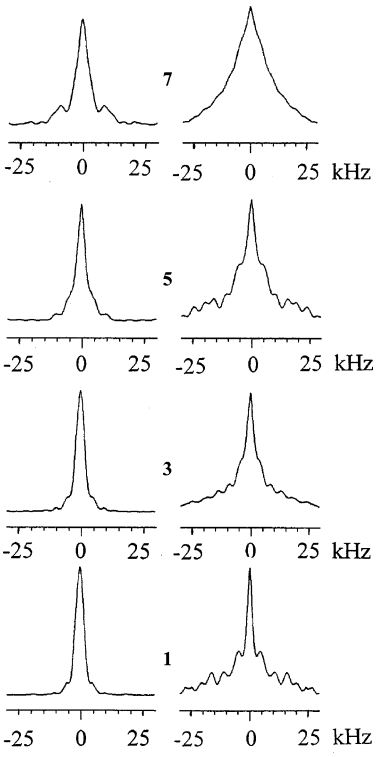

Figure 3. Dipolar cross sections for the PTMG $-OCH_2-$ (left) and amorphous PA $-CH_2-$ (right) resonances from samples **1**, **3**, **5**, and **7**. Same experimental conditions as in Figure 1.

widths of both types of methylene groups from the PTMG fragment are only representative of the most rigid fraction belonging to the soft component. The reverse sensitivity to the most mobile methylene groups from the PTMG blocks is exploited in proton spectra discussed below.

^{1}H MAS Spectra: Residual Proton−Proton Dipolar Broadening. High-resolution proton NMR spectroscopy is an inherently quantitative and sensitive probe of the hydrogen environment. In systems with not very tightly coupled protons, the spinning frequencies of a few kilohertz are usually sufficient to efficiently remove the residual dipolar broadening, which results in highly resolved proton spectra. Figure 4 shows the central part of ^{1}H MAS NMR spectra of PTMG2000 and of samples **1**−**7**, all acquired with a spinning frequency of 4 kHz. As expected, even with such a modest-speed MAS, a resolution of two PTMG resonance signals is easily available in all but one case. Indeed, the molecular mobility of the hard and soft blocks is so different at room temperature that two narrow resonance peaks are observed for $-CH_2-$ and $-OCH_2-$ from the PTMG fragments while the PA spectrum consists of a featureless broad line with a width of 30−40 kHz (not shown). More interestingly, Figure 4 shows progressively albeit not regularly increasing line broadening at higher PA/PTMG block length ratio. Indeed, while the residual dipolar broadening for **1** and **2** remains roughly the same as for PTMG with block length 2000, a substantial broadening is observed for **3** and **4**, for which the length ratio PA/PTMG has increased to one. Somewhat unexpectedly, the dipolar broadening effects are clearly less pronounced for sample **6** as compared with sample **5**, despite a 2-fold increase of the PA/PTMG ratio. The temperature dependence of ^{1}H spectra in poly(styrene-*block*-methylphenylsiloxane) (PS/PMPS), as compared with that of PMPS itself, has been used before by Cai et al.[38] to estimate the shift of T_g of the soft component. Such an approach would lead us to a somewhat unusual conclusion of decreasing T_g of the PTMG component when increasing the PA/PTMG ratio from two to four. Indeed, as we will show below, the observed effect is due to the presence of a small amount of highly mobile fraction in sample **6** and cannot be used as indicator of the glass transition temperature of the soft component as a whole.

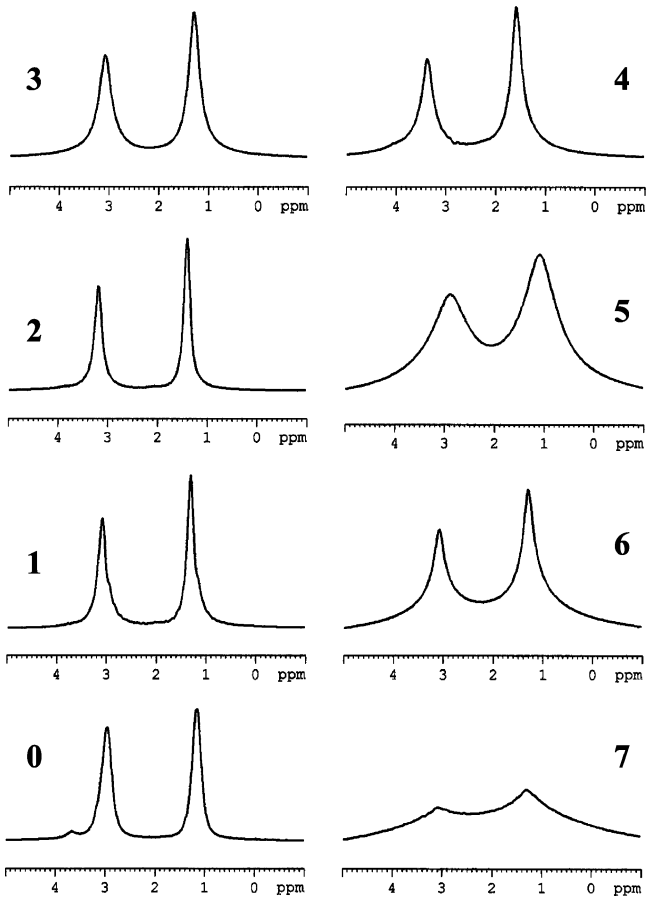

Figure 4. Central part of ^{1}H MAS (ν_r = 4 kHz) spectra of PTMG2000 (sample **0**) and PEBAX samples **1**−**7**.

^{13}C CP/MAS Spectra: Proton−Carbon J-Coupling Features. Heteronuclear *J*-resolved ^{13}C NMR spectra can be recorded in the solid state under a simultaneous application of magic-angle spinning and homonuclear proton decoupling.[39] In fact, when applying the homonuclear decoupling, the dipolar proton−proton interaction is averaged out, restoring the inhomogeneous character of the dipolar carbon−proton interaction. The effect of MAS is to narrow the inhomogeneously broadened lines due to the chemical shift anisotropy (CSA) and heteronuclear dipolar interactions. As a consequence, high-resolution liquidlike spectra can be obtained in the solid state, exhibiting scalar coupling and isotropic chemical shifts. In this experiment, however, the proton−carbon scalar coupling constants are scaled down by homonuclear proton decoupling. In some favorable conditions, MAS alone will be sufficient to reveal unscaled scalar ^{13}C−^{1}H couplings by averaging the homonuclear proton dipolar couplings and suppressing in this manner proton dipolar fluctuations modulating the heteronuclear scalar coupling interactions. This was indeed observed earlier in a cured, carbon black filled natural rubber.[40] Because of a high mobility of the

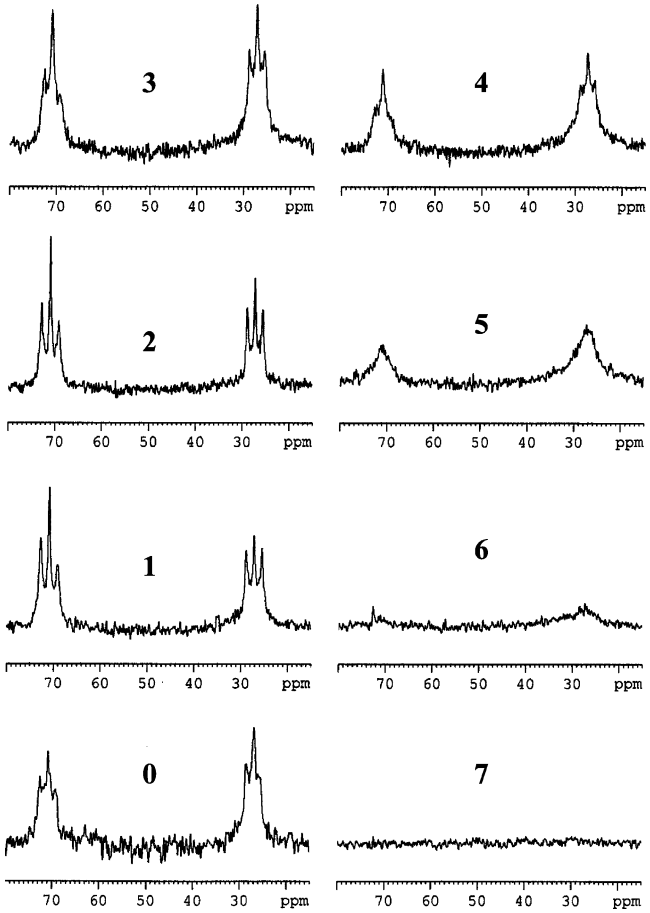

Figure 5. ^{13}C heteronuclear *J*-spectra of PTMG2000 (sample **0**) and samples **1**−**7** recorded without proton decoupling. All spectra have been recorded using CP contact time of 1 ms and with MAS at 4 kHz spinning.

PTMG, one can expect to get also such spectra in the case of poly(ether-*block*-amide) copolymers.

Figure 5 shows ^{13}C CP/MAS spectra (CT = 1 ms, ν_r = 4 kHz) of PTMG2000 and samples **1**−**7** recorded without heteronuclear decoupling. Well-resolved *J* multiplets can be observed for PTMG and samples **1**−**3**, while in the right-side spectra only sample **4** gives a hint of scalar effect. This reveals that, only in samples having the spectra with scalar effects, there exists a substantial fraction of carbons with residual anisotropic interactions small enough to be completely averaged by 4 kHz spinning, still being able to cross-polarize with 1 ms contact time. Noticeable differences, as compared with proton spectra shown in Figure 4, appear in the relation to decreasing mobility when going to higher PA/PTMG ratio or shorter length of soft blocks. Indeed, contrary to very similar proton spectra of samples **3** and **4**, a clearly smaller mobility is revealed in *J*-spectra when the length of each block is divided by two. This may be equally due to the renforced anchoring effect of PA block and/or to a less pronounced mobility of shorter PTMG blocks. An another difference is visible for samples **5** and **6** for which an expected global decrease of mobility is apparent for the second sample from barely appearing hints of ^{13}C resonances, while a reverse conclusion could be drawn from the corresponding proton spectra due to the presence of a small amount of highly mobile fraction in sample **6**.

Indirect $T_2(^1H)$ Relaxation Measurements. The cross-polarization technique offers the possibility of investigating one nucleus indirectly by means of the other nucleus involved in the polarization transfer. The complementary advantages of high sensitivity and high chemical shift dispersion offered by ^1H and ^{13}C spins have been exploited previously in heterogeneous organic solids for indirect measurements of T_2 relaxation times of proton attached to various types of carbons.[41] The method was originally applied to the case of macromolecular materials endowed with a distribution of T_2 values due to the presence of components with different molecular mobilities.[41a] The pulse sequence used for the measurements of ^1H T_2 times via detection of the ^{13}C resonances starts with a 90° proton pulse followed by a variable time left for transverse proton relaxation.[41a,c] The ^{13}C magnetization is than created by standard CP procedure. A plot of the intensity of the ^{13}C signal is a representation of the proton signal in the time domain, from which a characteristic proton time constant T_2 may be extracted.

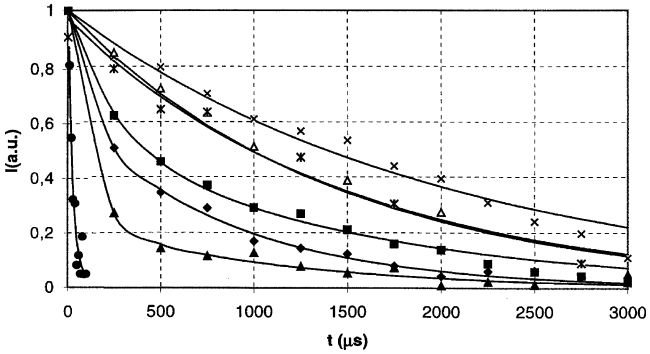

Figure 6. Temporal evolution of the ^{13}C resonance signal from the $-OCH_2-$ groups of PTMG in samples **1** (×), **2** (*), **3** (Δ), **4** (■), **5** (◆), **6** (▲), and **7** (●) as a function of time preceding the CP transfer (contact time CT = 1 ms).

Figure 6 shows such a temporal evolution of the ^{13}C resonance signal from the $-OCH_2-$ groups in samples **1**−**7** as a function of time preceding the CP transfer (contact time CT = 1 ms). Although the data as a whole visualize nicely progressively increasing transverse relaxation of these groups due to their decreasing overall molecular mobility when going from sample **1** to sample **7**, a single-exponential decay satisfactory fits the experimental data for samples **1**−**3** and **7**, while the presence of two relaxation processes had to be assumed for series **4**−**6**. This would mean the presence of single- and two-component character of PTMG blocks in the first and second group of samples, respectively. In fact, as will be shown in the second part of this paper, subtle fingerprints of motional heterogeneity of the PTMG blocks in the most mobile samples can be revealed by indirect $T_2(^1H)$ measurements using a range of CP contact times.

Indirect $T_{1\rho}(^1H)$ Relaxation Measurements. The measurements of spin−lattice relaxation in the rotating frame are frequently used to probe the spectral density of molecular motions in the mid-kilohertz range. However, through the spin-diffusion relaxation mechanism, proton $T_{1\rho}(^1H)$ can be strongly dependent on short-range spatial proximity of the interacting dipole moments of protons and thus very sensitive to the homogeneity of polymer systems.[42] To measure selectively proton $T_{1\rho}$ relaxation of each block, we again take advantage of indirect measurements via well-separated ^{13}C resonances of differently located methylene groups.

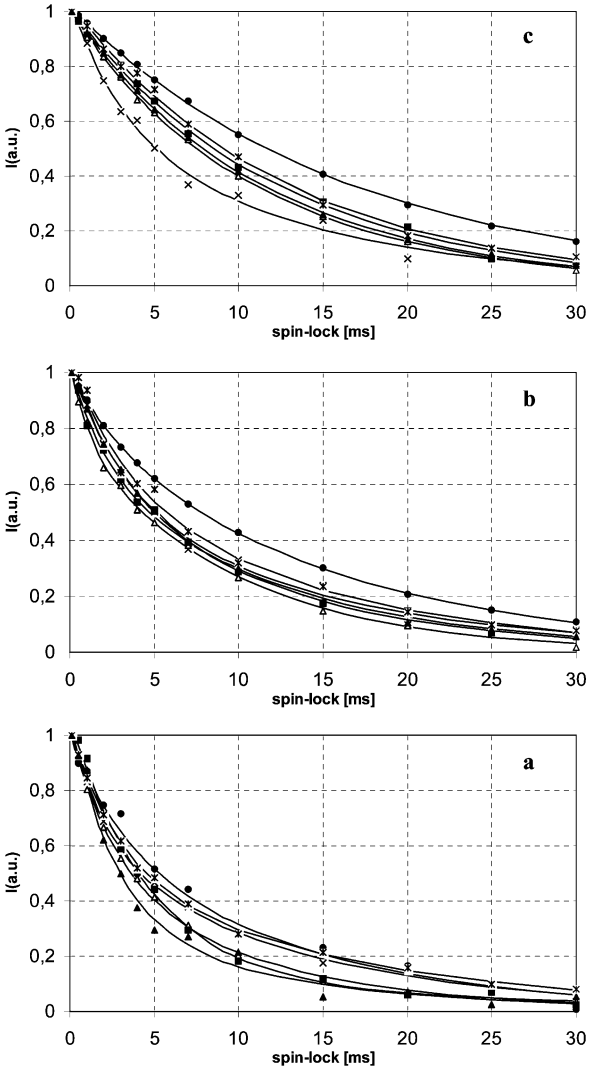

Figure 7. Indirect $T_{1\rho}(^1H)$ relaxation measurements for the $-OCH_2-$ groups of PTMG (a) and for the PA methylene belonging mostly to the amorphous (b) and crystalline (c) phases, respectively. Symbols are the same as in Figure 6. CT = 1 ms, ν_r = 4 kHz.

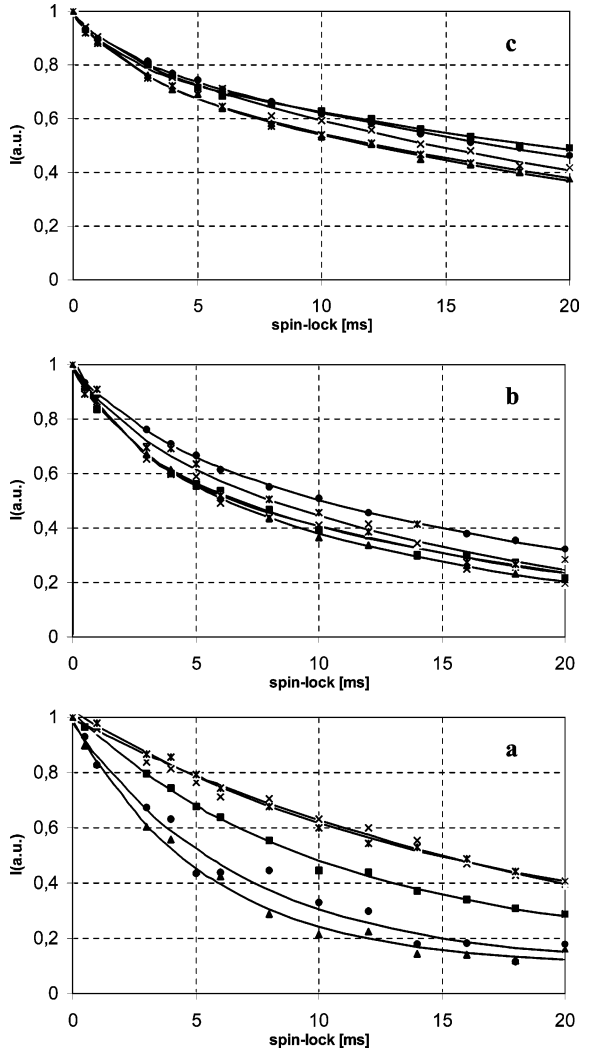

Figure 8. $T_{1\rho}(^{13}C)$ decays for the $-OCH_2-$ groups of PTMG (a) and for the PA methylene belonging mostly to the amorphous (b) and crystalline (c) phases, respectively. Symbols are the same as in Figure 6. CT = 1 ms, ν_r = 4 kHz.

Figure 7 shows three sets of relaxation curves for protons from $-OCH_2-$ groups of PTMG and from the PA methylene belonging mostly to the amorphous and crystalline phases. Somewhat surprisingly, roughly similar time constants of the relaxation decays are observed for these three spacial emplacements, without any regular dependence on the increasing PA/PTMG ratio or length of each block. This must be due to the averaging spin-diffusion effect. All temporal decays of the PTMG and the PA amorphous parts reveal a two-exponential relaxation, while monoexponential decays take place in all but one case (sample **1**) for amorphous trans−trans and crystalline emplacement. In the case of the PTMG protons, very similar time constants close to 2.6 ± 0.3 and 13.0 ± 2.0 ms come from samples **1**, **2**, **3**, **6**, and **7** while sample **4** shows somewhat eccentric behavior with two time constants equal to 4.8 and 27 ms. Consequently, the observed small differences in decays are mainly due to a somewhat different weighting of both processes. For the amorphous PA, except slightly slower relaxation in sample **7**, very similar time constants close to 2.8 ± 0.3 and 13.0 ± 2.0 ms are measured for all samples. Similarly, the slowest relaxation of trans−trans or crystalline protons is noted for sample **7**, while roughly half of this signal from sample **1** is relaxing more rapidly due to its actual provenance from the amorphous trans−trans fragments.

$T_{1\rho}(^{13}C)$ and $T_1(^{13}C)$ Relaxation Measurements. The rotating frame relaxation measurements for naturally abundant ^{13}C nuclei have also proved to be an efficient way of studying mid-kilohertz molecular motions in polymer systems.[43] However, the information on such motions is obtained only if the "spin−spin effect" is not the dominant one, i.e., if the fluctuations induced by the flip-flop terms of the proton−proton dipolar interaction have much more lower frequency than that of molecular motions.[44] This is the expected scenario for the soft component of the thermoplastic elastomers.

Indeed, contrary to the $T_{1\rho}(^1H)$ relaxation measurements, the $T_{1\rho}(^{13}C)$ decays (Figure 8a) of the $-OCH_2-$ signal from the PTMG blocks show increasing relaxation when going from the most mobile sample **1** to sample **6**, with the relaxation times changing from 21.8 to 5.3 ms for largely dominating (73−87%) fast relaxing fraction. This strongly suggests motional character of this relaxation parameter that seems to be in position to give a straightforward signature of the relative motional mobility of mobile fraction of the soft component. One can also note a somewhat slower relaxation rate in

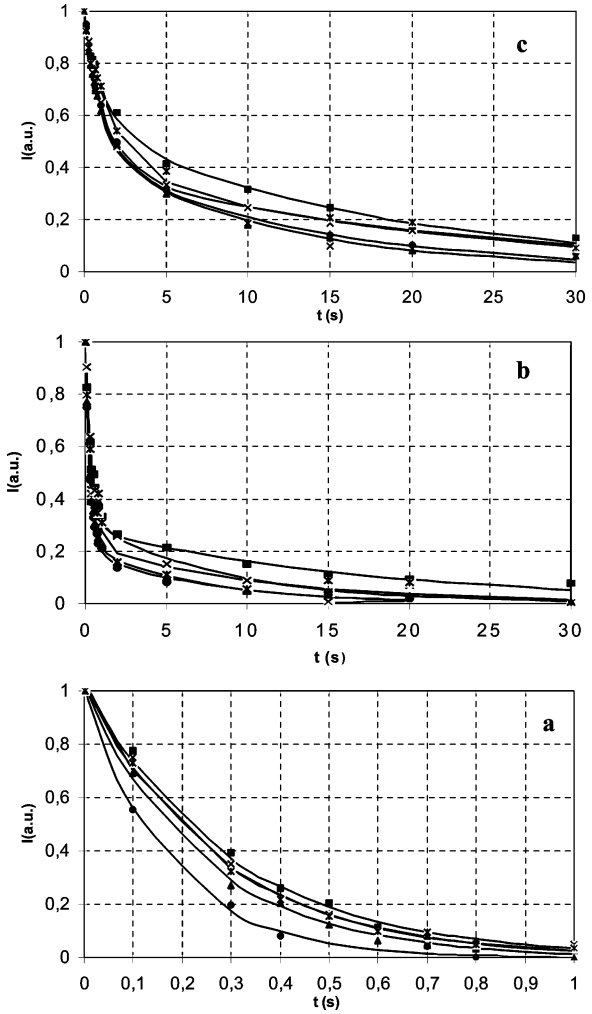

Figure 9. $T_1(^{13}C)$ decays for the $-OCH_2-$ groups of PTMG (a) and for the PA methylene belonging mostly to the amorphous (b) and crystalline (c) phases, respectively. Symbols are the same as in Figure 6. CT = 1 ms, ν_r = 4 kHz.

sample **7** as compared to the sample **6**. This suggests the passage through the highest spectral density of molecular motions with frequencies close to 60 kHz in sample **6** when going from sample **1** to sample **7**. For the amorphous PA (Figure 8b), and in analogy to $T_{1\rho}(^1H)$ relaxation measurements, very similar time constants close to 2.3 ± 0.3 and 17.0 ± 2.0 ms are measured for all but the most rigid sample. Two-exponential relaxation also governs the decays of carbons placed in the amorphous trans−trans fragments or crystalline phase of the PA (Figure 8c). Because of a roughly constant, minor amount (ranging between 13% in sample **1** to 22% in sample **6**) of rapidly relaxing fraction and given its relaxation parameter identical to that measured for the amorphous carbons of the PA, we assign this fraction to the amorphous PA blocks with trans−trans conformations.

The short $T_1(^{13}C)$ values of about 0.27 ± 0.3 s measured for the soft component are indicative of the presence of substantial spectral density of molecular motions in the megahertz frequency range, without any dependence on the mole fraction of hard segments or length of soft segments. However, in contrast to $T_{1\rho}$ relaxation measurements presented above, single-exponential decays govern the temporal evolution of magnetization in $T_1(^{13}C)$ relaxation measurements of the PTMG blocks in all samples (Figure 9a). This must

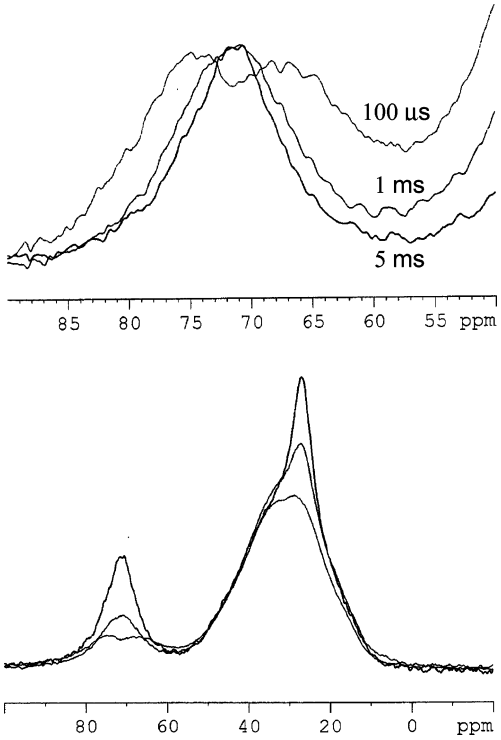

Figure 10. Static ^{13}C spectra of sample **3** recorded at three contact times of 100 μs, 1 ms, and 5 ms. For better comparison of the line shape, the expanded signals of the OCH_2 groups are shown with the same intensity on the top part of the figure.

be due to the preponderant averaging effect of spin diffusion, which manifests fully on the time scale of a few hundred milliseconds. This is supported by a somewhat unexpected fastest relaxation in the most rigid sample **7**, which offers the best conditions to the efficient spin exchange. However, clear two-exponential decays are systematically observed for both amorphous and crystalline emplacement of the PA carbons (Figure 9b,c). This brings immediately evidence of the large dimensions of the corresponding macroscopically separated regions.

3. Further Investigation of Motional Heterogeneity of the Soft Component. Although each type of spectra or relaxation measurements presented above shows specific, more or less pronounced sensitivity to overall structural ↔ motional changes, the subtle features of the revealed dynamic heterogeneity of the soft component remain difficult to appreciate and in some cases could be wrongly interpreted or simply overlooked. To get a deeper insight into the motional heterogeneity of this component, we chose to take advantage of the dependence of cross-polarization transfer efficiency on the strength of heteronuclear dipolar couplings governed by the extent of motional averaging. For this, we start with a simple visualization of expected motional distribution of the soft component, by recording a couple of static carbon-13 spectra at different CP contact times and comparing the resulting line shapes of individual resonances. As an example, Figure 10 shows the static spectra of sample **3** recorded at three contact times of 100 μs, 1 ms, and 5 ms. Although the observed changes of the line shape in the resonance region between 10 and 50 ppm visualize mainly an obvious, much more higher mobility of $-CH_2-$ type groups in the PTMG fragment as compared with such groups in the PA part, the dramatic changes of the line shape between 60 and 90 ppm, representing the

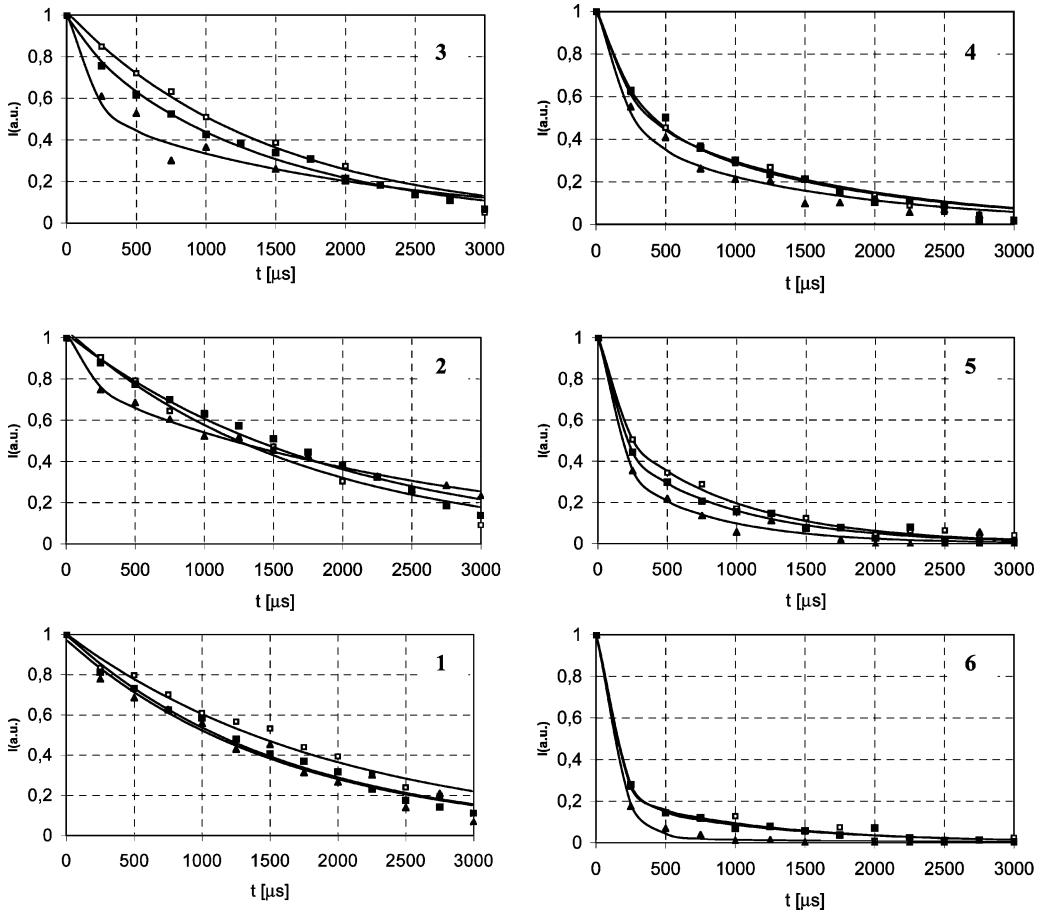

Figure 11. Indirect $T_2(^1H)$ relaxation measurements for the $-OCH_2-$ groups of PTMG in samples **1**−**6** recorded with three CP contact times of 100 μs (▲), 500 μs (■), and 1 ms (□).

$-OCH_2-$ groups of the soft component, give immediately evidence for the presence of distribution of heteronuclear dipolar couplings within these groups. This must be due to the dynamic heterogeneity encompassing relatively rigid fragments and much more highly mobile units as revealed at 100 μs and 5 ms contact times, respectively. Consequently, the observed changes strongly speak in favor of using a range of contact times as a sensitive contrast factor to probe motional heterogeneity of the soft component. However, as the static CP spectra clearly suffer from lower sensitivity and resolution as compared with CP/MAS spectra, all measurements presented below were obtained in the conditions of magic-angle rotation.

Cross-Polarization Filtered Indirect T_2 (^1H) Measurements. Here we come back to the selective measurements of proton transverse relaxation through the ^{13}C resonance signal of the $-OCH_2-$ group. Figure 11 shows the decays of magnetization for each sample recorded with three CP contact times of 100 μs, 500 μs, and 1 ms. For the most soft sample **1**, only monoexponential decays are detected; however, the decay constant increases from 1.6 ms at the first two contact times to 2.0 ms at the longest contact time. This is the indication of an inherent distribution of the residual proton−proton dipolar interactions, possible due to the anchoring effect of crystalline PA regions on neighboring PTMG blocks.

A substantial difference with a clear two-exponential decay at short contact time is observed when going to samples **2** and **3**. This reveals the presence of significantly restricted fraction, which can only be detected when using a short contact time filtering largely dominating highly mobile component. A clear fingerprint of the motional heterogeneity shows up also for samples **4**−**6**. Two-exponential decays are again systematically present with the first relaxation constant stretching respectively between 0.19−0.25, 0.1−0.12, and 0.1−0.14 ms, the second close to 1.5, 0.8, and 1.0 ms. Somewhat strangely, a small amount of highly mobile fraction with a relaxation constant of 2.0 ms is detected in sample **6** at short contact time. This nicely corroborates early mentioned less pronounced dipolar broadening effects observed in ^1H MAS spectra for sample **6** as compared with sample **5** (Figure 4).

Cross-Polarization Inversion Measurements. The method of selective polarization inversion of resonance signals depending on the polarization transfer rates between protons and rare spins was originally proposed by Melchior[45] and is now well established as one of the simplest tools for solid-state spectral editing. In this simple experiment the preparation period consists of the classical cross-polarization procedure, followed by a variable contact time with inverted phase of proton spin-locking irradiation. This leads to polarization inversion of ^{13}C spin magnetization. It has been demonstrated that the method is also very sensitive to the local mobility of different functional groups or sites in polymers.[46,47] Here we wish to exploit such a dynamic sensitivity of cross-polarization inversion measurements to test and exploit yet an another way to access the motional heterogeneity of the soft component.

The experimental data provided by the experiment run at four different contact times preceding variable cross-polarization inversion (CPI) period are shown in

Figure 12. No particular differences in the time of passage through zero intensity are noted for CPI curves recorded at short contact time of 100 μs. This proves the presence of small fraction with similar rigidity in all samples. Much slower CPI rates are observed when using longer contact times. This is due to the effective cross-polarization of much mobile fraction having smaller heteronuclear couplings combined with its increasing contribution to the observed signal when going to longer contact times. The data as a whole visualize the relative extent of motional heterogeneity of the soft component, which is the most pronounced albeit roughly similar for samples **1**−**3**, while a significant decrease of such an extent is observed for the three remaining samples. Equally interesting, despite 2-fold increase of the block length PA/PTMG ratio when going from sample **4** to sample **5**, clearly larger motional heterogeneity is observed for the more mobile fraction in sample **5**, which corroborates the $T_2(^1H)$ data (Figure 11) further discussed below.

General Discussion and Conclusions

The presented experimental results provide complementary information on the extent and differences of molecular mobility within a series of structurally different poly(ether-*block*-amide) copolymers. On the basis of the relationship between motional and structural characteristics, this permits a better insight into the structural features of investigated thermoplastic elastomers. Local-field dipolar spectra carry a straightforward signature of microphase-separated morphology endowed with a strong mobility gradient due to the presence of a PA crystalline phase and noncrystalline phases consisting of separated PTMG and PA regions. The observed dipolar features of the PA component also give evidence for the presence of its motional heterogeneity. Albeit the dipolar PA slices in Figure 3 visualize decreasing relative proportion of softened PA phase when going from sample **1** to sample **6**, an exact determination of corresponding amounts is not available from such spectra.

^{1}H MAS spectra provide an another fingerprint of microphase-separated systems with domains having the mobility close to those of individual homopolymers. Although such spectra roughly show increasing broadening at higher PA/PTMG ratio, they are mainly sensitive to the presence of the most mobile fragments and can give a distorted vision of the soft component in the presence of its dynamic heterogeneity. ^{13}C spectra bearing proton−carbon *J*-coupling features appear to be more sensitive to the length of the soft blocks and seem to bring a proper visualization of their overall mobility.

Indirect $T_2(^1H)$ relaxation measurements at single contact time (Figure 6), besides showing increasing transverse relaxation of $-OCH_2-$ groups due to their decreasing overall molecular mobility when going from sample **1** to sample **7**, immediately reveal the dynamic heterogeneity of the soft component in samples with the PA/PTMG block length ratio equal to one or higher, while more detailed information on the extent of motional ditribution of PTMG is provided by variable cross-polarization filter (Figures 11 and 12). Figure 13 resumes these results in terms of percentage of mobile and restricted fraction and corresponding distribution of $T_2(^1H)$ relaxation times. Somewhat unexpectedly, the first graph shows that in samples **4** and **5**, despite the factor two in the corresponding PA/PTMG block length

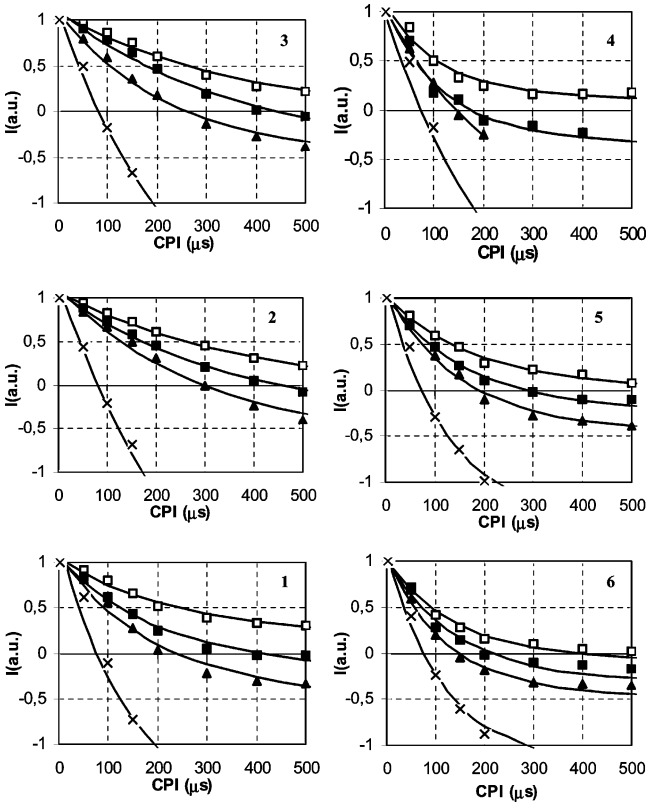

Figure 12. Changes in ^{13}C intensity of $-OCH_2-$ resonance signal for samples **1**−**6** in the cross-polarization inversion experiment using four different contact times preceding variable cross-polarization inversion (CPI) period: 100 μs (×), 500 μs (▲), 1 ms (■), and 5 ms (□).

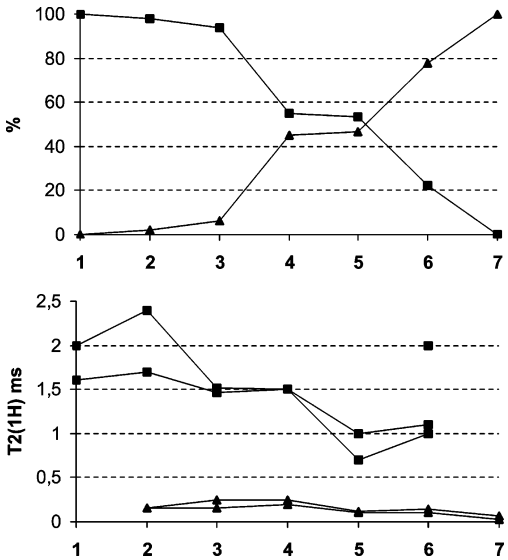

Figure 13. Relative percentage (a) of mobile (■) and restricted (▲) fraction within the soft component along with corresponding transverse relaxation constant times (b) as revealed by indirect $T_2(^1H)$ relaxation measurements from Figure 11.

ratio, roughly half of the soft component is present in the restricted state of both samples. It should be pointed out that a very similar percentage of mobile fraction in both samples does not imply the same mobility. Indeed, as shown in Figure 4, this fraction is more restricted in sample **5**, albeit its residual dipolar strength heterogeneity is more pronounced (Figure 13) than in sample **4**. This last feature is confirmed by the cross-polarization inversion data shown in Figure 12 despite a somewhat complicating effect arising from longer $T_{1\rho}(^1H)$ relax-

ation in sample **4**. Indeed, the cross-polarization inversion experiments provide, from the heteronuclear dipolar interaction perspective, an another visualization of the extent of motional ditribution of PTMG component. Interestingly, identical temporal evolution of the cross-polarization inversion curves recorded at the short contact time of 100 μs can be observed in all cases. We assign this characteristic feature to the anchoring effect of PA blocks on the outermost parts of the PTMG segments.

Finally, coming back to the variable cross-polarization $T_2(^1H)$ relaxation data exploited in Figure 13, a somewhat higher mobility of mobile PTMG fraction is observed when going from sample **5** to sample **6**, along with reappearance of a small population (~3%) of much more mobile fragments, observed earlier at higher proportion in softer samples **3** and **4**. The presence of this small amount of highly mobile fraction fully explains the apparent motional anomaly in ^1H MAS spectra (Figure 4) of samples **5** and **6**.

Very similar $T_{1\rho}(^1H)$ relaxation parameters have been revealed in all samples for three main spacial emplacements, i.e., within the soft PTMG, amorphous, and crystalline PA phases. From the point of view of these measurements, the overall mobility of each sample appears as having a two-component character, without any sensitivity to changes in the mobility of the soft component vs the PA/PTMG ratio. This strongly suggests the dominant effect of proton spin diffusion leading to a truncated spectroscopic response of two-component materials without any clear distinction between the PTMG and PA segments. On the contrary, apparently dominating motional character of the $T_{1\rho}(^{13}C)$ relaxation parameters of the PTMG $-OCH_2-$ carbons seems to be in a position to give a straightforward signature of the relative mobility of mobile fraction of the soft component, however, without any sensitivity to the amount of its restricted fraction. This must be due once again to the averaging spin-diffusion effect.

Summing up, subtle spectroscopic fingerprints of the dynamic heterogeneity of the soft component in poly(ether-*block*-amide) copolymers can be observed by exploiting the indirect $T_2(^1H)$ relaxation measurements at different cross-polarization contact times. We believe that the revealed fingerprints and the ways exploited in this work for their retrieval might be helpful for a better assessment of its role in the mechanical properties of thermoplastic elastomers.

References and Notes

(1) (a) Holden, G.; Legge, N. R.; Quirk, R.; Schroeder, H. E. *Thermoplastic Elastomers, A comprehensive review*, 2nd ed.; Hanser: Munich, 1996, and references therein. (b) Eustache, R.-P. In *Handbook of Condensation Thermoplastic Elastomers*; Fakirov, S., Ed.; Wiley-VCH Verlag GmbH & Co.: Berlin, 2005; Chapter 10.
(2) Xie, M.; Camberlin, Y. *Makromol. Chem.* **1986**, *187*, 383.
(3) (a) Sauer, B. B.; Mclean, R. S.; Brill, D. J.; Londono, D. J. *J. Polym. Sci., Part B: Polym. Phys*. **2002**, *40*, 1727. (b) Sauer, B. B.; Mclean, R. S.; Thomas, R. R. *Polym. Int.* **2000**, *49*, 449.
(4) Sheth, J. P.; Xu, J.; Wilkes, G. L. *Polymer* **2003**, *44*, 743.
(5) Okoroafor, E.; Rault, J. *J. Polym. Sci., Part B: Polym. Phys.* **1991**, *29*, 1427.
(6) (a) Di Lorenzo, M. L.; Pyda, M.; Wunderlich, B. *J. Polym. Sci., Part B: Polym. Phys.* **2001**, *39*, 1594. (b) Di Lorenzo, M. L.; Pyda, M.; Wunderlich, B. *J. Polym. Sci., Part B: Polym. Phys.* **2001**, *39*, 2969.
(7) Ghosh, S.; Khastgir, D.; Bhowmick, A. K. *Polymer* **1998**, *39*, 3967.
(8) Faruque, H. S.; Lacabanne, C. *Polymer* **1986**, *27*, 527.
(9) (a) Assink, R. A.; Wilkes, G. L. *Polym. Eng. Sci.* **1977**, *17*, 606. (b) Assink, R. A. *Macromolecules* **1978**, *11*, 1233.
(10) Lind, A. C. *J. Chem. Phys.* **1977**, *66*, 3482.
(11) (a) Tanaka, H.; Nishi, T. *J. Chem. Phys.* **1985**, *82*, 4326. (b) Tanaka, H.; Nishi, T. *Phys. Rev. B* **1986**, *33*, 32.
(12) Colquhoun, I. J.; Packer, K. J. *Br. Polym. J.* **1987**, *19*, 151.
(13) Clauss, J.; Schmidt-Rohr, K.; Spiess, H. W. *Acta Polym.* **1993**, *44*, 1.
(14) Weigand, F.; Demco, D. E.; Blümich, B.; Spiess, H. W. *J. Magn. Reson. A* **1996**, *120*, 190.
(15) (a) Wang, J.; Jack, K. S.; Natansohn, A. L. *J. Chem. Phys.* **1997**, *107*, 1016. (b) Jack, K. S.; Wang, J.; Natansohn, A.; Register, R. A. *Macromolecules* **1998**, *31*, 3282. (c) Neagu, C.; Puskas, J. E.; Singh, M. A.; Natansohn, A. *Macromolecules* **2000**, *33*, 5976. (d) Yu, H.; Natansohn, A.; Singh, M. A.; Torriani, I. *Macromolecules* **2001**, *34*, 1258.
(16) Lehmann, S. A.; Meltzer, A. D.; Spiess, H. W. *J. Polym. Sci., Part B: Polym. Phys.* **1998**, *36*, 693.
(17) De Paul, S. M.; Zwanziger, J. W.; Ulrich, R.; Wiesner, U.; Spiess, H. W. *J. Am. Chem. Soc.* **1999**, *121*, 5727.
(18) Kretschmer, A.; Drake, R.; Neidhoefer, M.; Wilhelm, M. *Solid State Nucl. Magn. Reson.* **2002**, *22*, 204.
(19) Litvinov, V. M.; Bertmer, M.; Gasper, L.; Demco, D. E.; Blümich, B. *Macromolecules* **2003**, *36*, 7598.
(20) Hou, S.-S.; Bonagamba, T. J.; Beyer, F. L.; Madison, P. H.; Schmidt-Rohr, K. *Macromolecules* **2003**, *36*, 2769.
(21) Buda, A.; Demco, D. E.; Bermer, M.; Blümich, B.; Reining, B.; Keul, H.; Höcker, H. *Solid State Nucl. Magn. Reson.*. **2003**, *24*, 39.
(22) Stöppelmann, G.; Gronski, W. *Polymer* **1990**, *31*, 1838.
(23) Meltzer, A. D.; Spiess, H. W.; Eisenbach, C. D.; Hayen, H. *Macromolecules* **1992**, *25*, 993.
(24) Nakajima, T.; Akiyama, T.; Furuya, H. *Magn. Reson. Chem.* **2002**, *40*, 161.
(25) (a) Lorthioir, C.; Auroy, P.; Deloche, B.; Gallot, Y. *Eur. Phys. J. E* **2002**, *7*, 261. (b) Lorthioir, C.; Auroy, P.; Deloche, B. *Eur. Phys. J. E* **2003**, *11*, 3.
(26) (a) Jelinski, L. W.; Schilling, F. C.; Bovey, F. A. *Macromolecules* **1981**, *14*, 581. (b) Jelinski, L. W.; Dumais, J. J.; Engel, A. K. *Macromolecules* **1983**, *16*, 403. (c) Jelinski, L. W.; Dumais, J. J.; Watnick, P. I.; Engel, A. K.; Sefcik, M. D. *Macromolecules* **1983**, *16*, 409.
(27) (a) Klug, C. A.; Wu, J. Xiao, C.; Yee, A. F.; Schaefer, J. *Macromolecules* **1997**, *30*, 6302. (b) Liu, J.; Goetz, J. M.; Schaefer, J.; Yee, A. F.; Li, L. *Macromolecules* **2001**, *34*, 2559.
(28) Gabriëlse, W.; Soliman, M.; Dijkstra, K. *Macromolecules* **2001**, *34*, 1685.
(29) Bertmer, M.; Gasper, L.; Demco, D. E.; Blümich, B.; Litvinov, V. M. *Macromol. Chem. Phys.* **2004**, *205*, 83.
(30) Hatfield, G. R.; Guo, Y.; Killinger, W. E.; Andrejak, R. A.; Roubicek, P. M. *Macromolecules* **1993**, *26*, 6350.
(31) Boulares, A.; Tessier, M.; Maréchal, E. *Polymer* **2000**, *41*, 3561.
(32) Torchia, D. A. *J. Magn. Reson.* **1978**, *30*, 613.
(33) Schmidt-Rohr, K.; Clauss, J.; Spiess, H. W. *Macromolecules* **1992**, *25*, 3273.
(34) Palmas, P.; Tekely, P.; Canet, D. *Solid State NMR* **1995**, *4*, 105.
(35) Takegoshi, T.; McDowell, C. A. *J. Magn. Reson.* **1986**, *66*, 14.
(36) Malveau, C.; Tekely, P.; Canet, D. *Solid State NMR* **1997**, *7*, 271.
(37) Tekely, P.; Palmas, P.; Mutzenhardt, P. *Macromolecules* **1993**, *26*, 7363.
(38) Cai, W. Z.; Schmidt-Rohr, K.; Egger, N.; Gerharz, B.; Spiess, H. W. *Polymer* **1993**, *34*, 267.
(39) Terao, T.; Miura, H.; Saika, A. *J. Chem. Phys.* **1981**, *75*, 1573.
(40) Kentgens, A. P. M.; Veeman, W. S.; van Bree, J. *Macromolecules* **1987**, *20*, 1234.
(41) (a) Tekely, P.; Nicole, D.; Brondeau, J.; Delpuech, J. J. *J. Phys. Chem.* **1986**, *90*, 5608. (b) Tekely, P.; Vignon, M. R. *J. Polym. Sci., Part C: Polym. Lett.* **1987**, *25*, 257. (c) Tekely, P.; Canet, D.; Delpuech, J. J. *Mol. Phys.* **1989**, *67*, 81.
(42) Tekely, P.; Lauprêtre, F.; Monnerie, L. *Polymer* **1985**, *26*, 1081.
(43) Schaefer, J.; Sefcik, M. D.; Stejskal, E. O.; McKay, R. A. *Macromolecules* **1984**, *17*, 1118.
(44) Tekely, P.; Canet, D.; Delpuech, J. J.; Virlet, J. *Magn. Reson. Chem.* **1990**, *28*, 10.
(45) Melchior, M. T. Presented at the 22nd Experimental NMR Conference, Poster B-29, Asilomar, 1981.
(46) Cory, D. G.; Ritchey, W. M. *Macromolecules* **1989**, *22*, 1611.
(47) (a) Tekely, P.; Delpuech, J. J. *Fuel* **1989**, *68*, 947. (b) Tekely, P.; Montigny, F.; Canet, D.; Delpuech, J. J. *Chem. Phys. Lett.* **1990**, *175*, 401.

MA051625Q